

Role of $\alpha 9$ Nicotinic ACh Receptor Subunits in the Development and Function of Cochlear Efferent Innervation

Douglas E. Vetter,^{1,7} M. Charles Liberman,² Jeffrey Mann,³ Jacques Barhanin,⁴ Jim Boulter,⁵ M. Christian Brown,² Joanne Saffiote-Kolman,¹ Stephen F. Heinemann,¹ and A. Belén Elgoyhen⁶

¹The Salk Institute for Biological Studies
La Jolla, California 92037

²Eaton-Peabody Laboratory
Massachusetts Eye and Ear Infirmary
and Department of Otology and Laryngology
Harvard Medical School
Boston, Massachusetts 02114

³Beckman Research Institute
of the City of Hope
Duarte, California 92010

⁴Centre National de la Recherche Scientifique
Institut de Pharmacologie Moléculaire et Cellulaire
Sophia Antipolis 06560
Valbonne
France

⁵Department of Psychiatry
and Biobehavioral Sciences
University of California, Los Angeles
Los Angeles, California 90095

⁶Instituto de Investigaciones en Ingeniería
Genética y Biología Molecular
CONICET-UBA
Buenos Aires 1428
Argentina

Summary

Cochlear outer hair cells (OHCs) express $\alpha 9$ nACh receptors and are contacted by descending, predominantly cholinergic, efferent fibers originating in the CNS. Mice carrying a null mutation for the nACh $\alpha 9$ gene were produced to investigate its role(s) in auditory processing and development of hair cell innervation. In $\alpha 9$ knockout mice, most OHCs were innervated by one large terminal instead of multiple smaller terminals as in wild types, suggesting a role for the nACh $\alpha 9$ subunit in development of mature synaptic connections. $\alpha 9$ knockout mice also failed to show suppression of cochlear responses (compound action potentials, distortion product otoacoustic emissions) during efferent fiber activation, demonstrating the key role $\alpha 9$ receptors play in mediating the only known effects of the olivocochlear system.

Introduction

The end organs of the inner ear transduce acoustic stimuli, head accelerations, and body position relative to the gravitational force. It has been known for many years that the auditory epithelia are targets of a descending

efferent innervation originating from the superior olivary complex, located in the brainstem (Rasmussen, 1942, 1946, 1955). The functional significance of this olivocochlear (OC) system, however, has remained controversial. The OC system can be divided into lateral and medial subsystems, with different central origins and peripheral projections and targets. Lateral OC neurons project primarily to the spiral ganglion cell dendrites, which contact inner hair cells (IHCs), whereas medial OC neurons project directly onto outer hair cell (OHC) somata. The primary neurotransmitter used by both the lateral and medial OC systems is acetylcholine (ACh), although other neurotransmitters and modulators have been detected in lateral OC neurons, including GABA, CGRP, and opioid peptides (for review, see Eybalin, 1993). A number of nicotinic ACh receptor subunits (but not $\alpha 9$) are expressed by sensory neurons of the spiral ganglion (Hiel et al., 1996; Morley et al., 1998), and their activity may thus directly modulate neural activity of the ganglion cells. On the other hand, the $\alpha 9$ nicotinic receptor subunit appears to be the only nicotinic receptor subunit expressed by hair cells and, thus, is in a position to influence both hair cell presynaptic activity and cochlear mechanics.

Electrical stimulation of OC fibers has been shown to elevate cochlear thresholds (Galambos, 1956; Wiederhold and Kiang, 1970; Klinke and Galley, 1974; Brown and Nuttall, 1984) and suppress the mechanical response of the basilar membrane to auditory stimuli (Mountain, 1980; Murugasu and Russell, 1996; Ulfendahl, 1997). These observations are consistent with theories that (1) OHCs act as mechanical amplifiers enhancing basilar-membrane motion and (2) OC suppressive effects are mediated via terminals of the medial OC system that synapse on OHCs. Pharmacological studies further suggest that OC effects in the cochlea are mediated via $\alpha 9$ -containing receptors since, *in vivo*, blocker specificity (Kujawa et al., 1992, 1994) is similar to that reported for $\alpha 9$ receptors expressed in oocytes (Elgoyhen et al., 1994). Thus, the medial OC system appears to be a gain-control system, possibly mediated by $\alpha 9$ receptors expressed by OHCs. The peripheral effects of the lateral OC innervation of sensory neurons remain enigmatic.

Olivocochlear fibers reach the mouse otocyst very early in development (E12) (Fritzsche and Nichols, 1993). Although prior to birth these fibers are still morphologically immature, they are biochemically differentiated, expressing both choline acetyltransferase and acetylcholinesterase (Emmerling et al., 1990). $\alpha 9$ gene expression, however, is first detected at E18 in cochlear hair cells (Luo et al., 1998). Therefore, when $\alpha 9$ expression begins, ligands are probably available to activate the $\alpha 9$ nicotinic receptor. Since the efferent fibers first arrive at a still actively developing otocyst at a time when the auditory system is not yet functional, neurotransmitters released from the efferent system and the receptors that transduce this activity, that is, $\alpha 9$, could play a role in inner ear development. Experiments on neonatal cochlear deafferentation provide some evidence for this

⁷To whom correspondence should be addressed (e-mail: vetter@salk.edu).

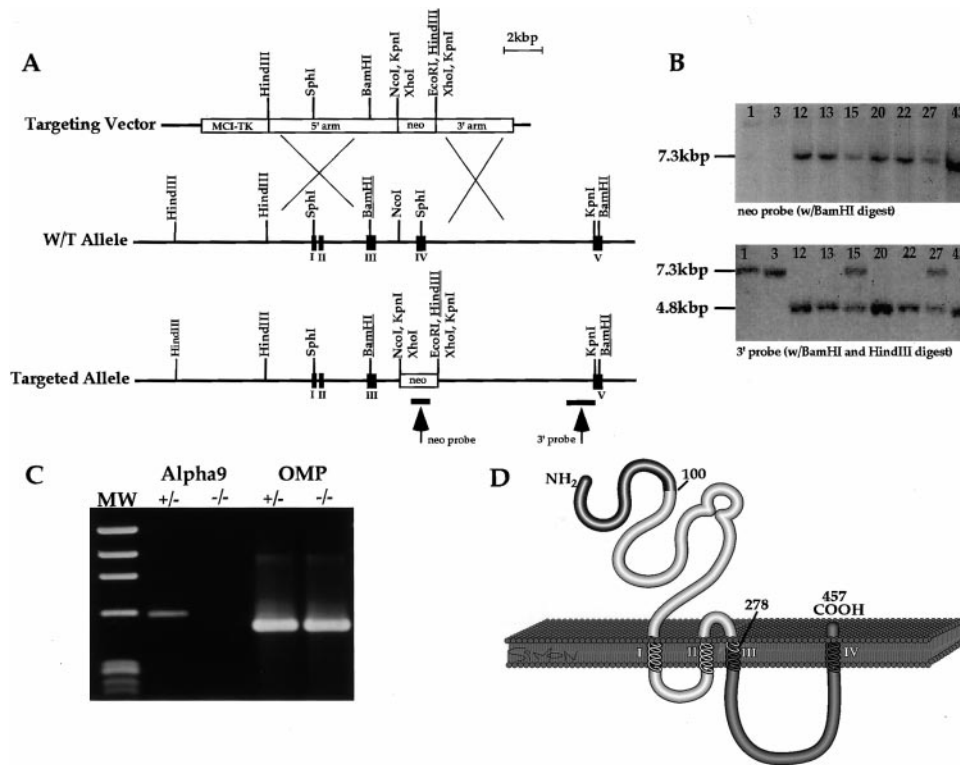


Figure 1. Targeted Disruption of the $\alpha 9$ Gene

(A) Gene structures and restriction maps for the $\alpha 9$ -targeting construct and wild-type and recombinant alleles are shown. Black boxes represent the exons of the $\alpha 9$ gene. Exon 4 of the wild-type allele is replaced by a neomycin resistance gene (*neo*), and the herpes simplex virus thymidine kinase gene (MC1-TK) is attached at the 5' end of the targeting vector for the purposes of negative selection. The locations of the 3' flanking and neomycin cassette probes are indicated (3' probe and *neo* probe, respectively). Restriction sites underlined indicate sites used for genotyping animals.

(B) Southern blot analysis of tail genomic DNA isolated from mice. The upper panel shows a Southern blot in which a probe for the neomycin cassette was used to hybridize the isolated DNA following a BamHI digest. Only DNA from mice that carry at least one copy of the mutant $\alpha 9$ allele can test positively. The predicted fragment size of 7.3 kbp was observed in these cases. The lower panel shows a Southern blot in which the 3' probe was used to genotype mice following a BamHI-HindIII digest of isolated DNA. Wild-type mice possess no *neo* band in the upper panel, and only a 7.3 kbp fragment in the lower panel (samples 1 and 3). Heterozygous mice possess both a *neo* band in the upper panel and two bands (a 7.3 kbp band and a 4.8 kbp band) in the lower panel (samples 15 and 27), while homozygous mice possess a *neo* band and only a 4.8 kbp band in the lower panel (samples 12, 13, 20, 22, and 43).

(C) RT-PCR analysis for $\alpha 9$ expression in olfactory tissue from heterozygous and knockout $\alpha 9$ mice is shown. Additionally, RT-PCR analysis using primers specific for the olfactory marker protein (OMP) are shown to illustrate that the RNA isolated from these mice is of high quality for use as template for RT-PCR reactions. $\alpha 9$ heterozygous mice possess a fragment of the predicted size (594 bp), while no band is observed with RNA isolated from the homozygous knockout mice. The predicted size of the band from the homozygous mice is 61 bp and has run off the gel. These results confirm that exon 4 is not present in the homozygous knockout mice.

(D) Schematic of the $\alpha 9$ protein shows the region of the protein involved by the recombination event. The first 100 amino acids of the protein are represented as a black and white segment and are not involved in the recombination events. The *neo* cassette replaced the region of the gene encoding the ligand-binding site, the entire first and second transmembrane domains, and a portion of the third transmembrane domain (amino acids 100–278; lightly shaded region). The final region of the protein, not directly involved with the recombination process, is shaded dark gray. However, due to a frame shift imposed by the incorporation of the targeting vector and the stop codons within the *neo* cassette itself, this region is not capable of coding for $\alpha 9$ protein expression. Additionally, at least one nonnative stop codon is introduced following the third transmembrane domain as a result of the frameshift.

(Walsh et al., 1998). Such a developmental role for $\alpha 9$ may include transducing early ACh release as signals that alter gene expression and/or cell growth, rather than as classical neurotransmission signals. The idea that neurotransmitters participate in developmental or morphogenetic signaling roles prior to their role in conventional neurotransmission has been previously suggested (Lauder, 1993). For instance, ACh has been implicated as a regulator of neurite extension in both the retina (Lipton et al., 1988) and hippocampus (Mattson, 1988).

To investigate the role(s) of the $\alpha 9$ nicotinic ACh receptor subunit in vivo, both in developmental processes and adult auditory function, we used a gene-targeting strategy to generate a mouse strain homozygous for a null mutation of the $\alpha 9$ gene. This report describes the production of the $\alpha 9$ knockout mouse, as well as an anatomical and physiological characterization of this mouse, and describes the consequences of $\alpha 9$ gene ablation for the overall development and function of the peripheral auditory system.

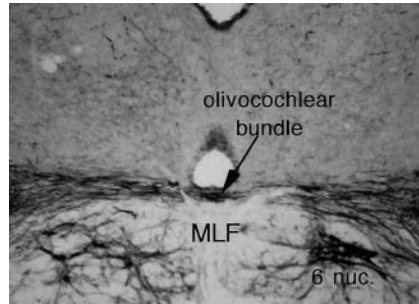


Figure 2. Choline Acetyltransferase Immunostaining of the Olivocochlear Bundle in $\alpha 9$ Knockout Mice

Frozen sections of a brain obtained from an $\alpha 9$ knockout mouse were processed for immunostaining using an antibody to ChAT to illustrate cholinergic fibers and cell bodies. A ChAT-positive fiber bundle (arrow) crossing the midline and occupying the area normally associated with the olivocochlear bundle in wild-type mice was consistently observed in three knockout mice. MLF, medial longitudinal fasciculus; 6 nuc, abducens nucleus. Magnification, 100.

Results

Generation and Analysis of $\alpha 9$ Mutant (Knockout) Mice

The intron-exon structure of the $\alpha 9$ gene obtained by genomic mapping is illustrated in Figure 1A. In the targeting construct, exon 4 and its flanking intronic sequences (including splice donor and acceptor sites) were replaced by a neomycin resistance gene. This renders any translated $\alpha 9$ protein nonfunctional, since exon 4 contains the coding sequence for the ligand-binding site, the first two transmembrane regions of the protein, including the pore region, and approximately half of the third transmembrane domain (Figure 1D). A BamHI/HindIII digest (Figure 1B) of mouse tail genomic DNA generated a 7.3 kbp fragment derived from the wild-type allele and the predicted 4.8 kbp fragment from the targeted allele. In addition, a BamHI digest generated the predicted 7.3 kbp fragment derived from the targeted allele as revealed with a probe specific for the neomycin cassette (Figure 1B). These results indicate correct integration of the targeting sequence within the $\alpha 9$ gene and production of viable mice carrying this $\alpha 9$ mutation. The complete absence of exon 4 in homozygous $\alpha 9$ knockout mice was verified by RT-PCR analysis of mRNA extracted from mouse nasal epithelium (Figure 1C), an easily accessible site of $\alpha 9$ gene expression (Elgoyhen et al., 1994). Thus, the generation of mice with a targeted disruption of the $\alpha 9$ gene can be demonstrated at both the DNA and RNA levels.

In addition to removing the ligand-binding site and the first two transmembrane domains, our construct disables the expression of sequence downstream from the neomycin cassette. The neomycin insertion generates a frameshift in the open reading frame, such that the remaining sequence (the second half of the third transmembrane domain, the intracellular loop, and the fourth transmembrane domain) is not translated, and introduces potential stop codons not found in the native open reading frame (area effected schematically illustrated in Figure 1D).

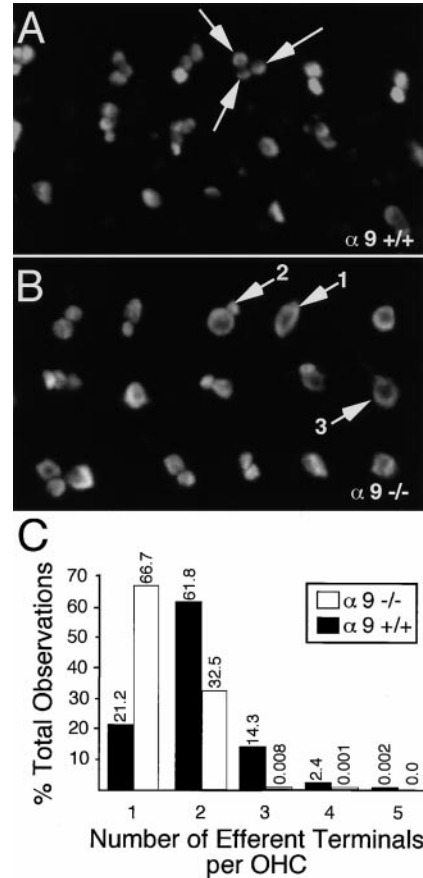


Figure 3. Olivocochlear Innervation of the OHC Region

The morphology of efferent terminals are compared between wild-type and knockout mice.

(A) Synaptophysin immunostaining of the OHC region in wild-type mice labels efferent terminals under OHCs. These terminals regularly occurred as clusters, such as the triplet indicated by the three arrows. Magnification, 1600.

(B) Synaptophysin immunostaining in knockout mice also shows efferent terminals under OHCs, but with abnormal morphology. In the knockout, most terminals occurred as singlets rather than as clusters (arrow 1) and associated terminals were often small in size (arrow 2). Terminals often showed a faint-staining center (arrow 3), which may reflect a hypertrophied synaptic terminal growing around the base of an OHC. Magnification, 1600.

(C) Descriptive analysis of the innervation to OHCs in wild-type and knockout mice. Note that (A) and (B) cannot be assumed to be representative of the population due to the small number of cells sampled in these micrographs. Counts of efferent terminals per OHC were taken from the middle turn of homozygous knockout mice and their littermate wild-type controls. Terminals were counted under 539 OHCs in wild type and 859 OHCs in knockouts.

The $\alpha 9$ knockout mice have no obvious phenotype based on external observation. The mice have a clear Preyer's reflex and have no obvious difficulties with balance or movement.

Cochlear Morphology and Efferent Innervation Patterns

Hair cells are the only cell population to express $\alpha 9$ in the organ of Corti, both in the adult (Elgoyhen et al., 1994; Glowatzki et al., 1995) and in utero (Luo et al.,

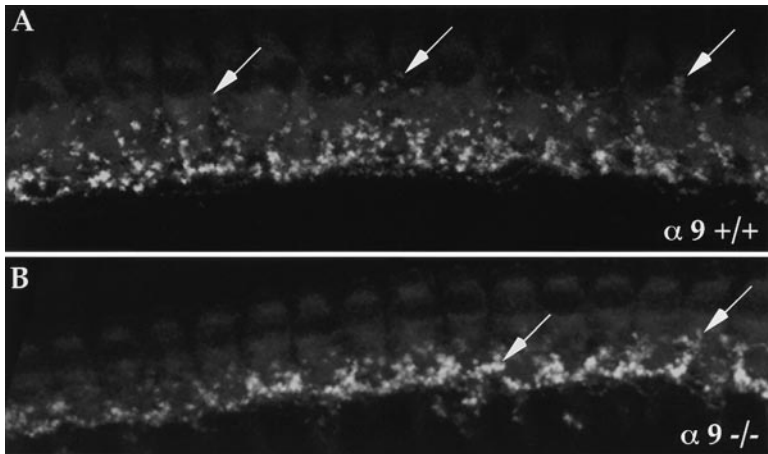


Figure 4. Olivocochlear Innervation of the IHC Region

(A) Synaptophysin immunostaining of efferent terminals under IHCs of wild-type mice revealed the expected dense plexus of terminals presumably contacting the radial fibers of the spiral ganglion below the hair cells, as well as a much sparser innervation of the IHC somata (arrows). Magnification, 750.

(B) Synaptophysin immunostaining of efferent terminals under IHCs of knockout mice revealed a plexus of terminals below the IHCs (arrows; compare with [A]). However, no terminal profiles were observed in close apposition to the IHC somata. Magnification, 745.

1998). A light-microscopic examination of cochlear sections stained with hematoxylin and eosin revealed no structural abnormalities in homozygous knockouts or heterozygous littermates anywhere in the cochlear duct, including the hair cells, their supporting cells, or in the spiral ganglion, where the cell bodies of primary sensory neurons are found (data not shown).

To assess the brainstem trajectory of the OC bundle, choline acetyltransferase (ChAT) immunostaining was performed on brainstem slices. In all three knockout mice examined, a ChAT-immunoreactive fiber bundle was observed crossing the midline in the expected location of the OC bundle, suggesting that the gross development and position of the OC bundle is not altered in the knockouts (Figure 2). This point is critical in interpreting our failure to elicit classic OC effects when electrically stimulating the brainstem in knockout mice (see below).

Cochlear efferent innervation was evaluated with antibodies specific for either (1) the vesicular acetylcholine transporter (VAT), to reveal cholinergic components, or (2) synaptophysin, an integral protein of the synaptic vesicle membrane, to reveal the overall efferent innervation.

In wild-type mice, synaptophysin-immunostained profiles were present along the entire cochlea, from base to apex, as (1) a regular array of larger terminals and terminal clusters in the OHC area, mirroring the pattern of the OHCs they contact (Figure 3A), and (2) a spiraling plexus of small terminals under the IHCs (Figure 4). In general, these differing innervations of the inner and outer hair cell areas correspond to the projections of lateral OC and medial OC subsystems, respectively. The distribution of VAT-immunostained terminals in the wild type (Figure 5) was qualitatively similar to that for synaptophysin, consistent with the view that the great majority of vesiculated (efferent) terminals in the organ of Corti are cholinergic.

Confocal microscopy of synaptophysin immunostaining revealed abnormalities in terminal morphology and number in the knockout mice (Figure 3B). In the OHC region of knockout mice, labeled terminals were fewer in number and larger in size compared to their wild-type littermates (Figures 3A and 3B). In the middle cochlear turn, the number of terminals per OHC (Figure 3C) in

wild types ranged from one to five, with most OHCs (61.8%) contacted by two terminals. In knockouts, most OHCs were contacted by only one terminal (66.7%) and very few by more than two (Figure 3C). A *t* test performed on the data showed that the difference between the mean number of terminals under hair cells of the wild-type mice (1.991) versus the knockouts (1.346) was significant at $p < 0.0001$ (with a standard error of 0.030 for the wild type and 0.037 for the knockout). Furthermore, in wild types, the terminals within a cluster were of roughly equal size (average, 3.1 μm), whereas in the knockout, the singlet terminals were larger (average, 6.5 μm) (Figures 3A and 3B). However, cochleas examined from wild-type mice always possessed some large singlet terminals under OHCs, and these terminals were approximately equal in average size to the more numerous large terminals found in the cochleas of knockout mice.

Confocal microscopy of synaptophysin-stained cochlea also revealed abnormalities in the IHC area (Figure 4). In wild types, the spiraling plexus of synaptophysin-positive terminals included a dense matrix at levels well below the IHC base, where terminals contact dendrites of primary sensory neurons (Slepecky, 1996), as well as a sparser plexus of terminals positioned around the IHC soma, sometimes at levels up to the nucleus (Figure 4A). The latter population of terminals, which may make synaptic contact with the IHC itself (Emmerling et al., 1990; Hashimoto et al., 1990; Sobkowicz, 1992), appears to be absent in the knockout (Figure 4B).

Finally, in the organ of Corti of $\alpha 9$ knockout mice, VAT immunostaining revealed a persistent cholinergic innervation, from base to apex in both IHC and OHC areas, despite the lack of the $\alpha 9$ subunit (Figures 5A and 5B). Additionally, the synaptic terminals under OHCs exhibited an unusual morphology similar to that observed following synaptophysin immunostaining (Figures 5A' and 5B').

Cochlear Function and Assays of OC Peripheral Effects

General cochlear sensitivity and function was assessed using distortion product otoacoustic emissions (DPOAEs) and compound action potentials (CAPs). The DPOAE assay is particularly useful in assessing the functional state of the OHCs. The normal ear creates a number of

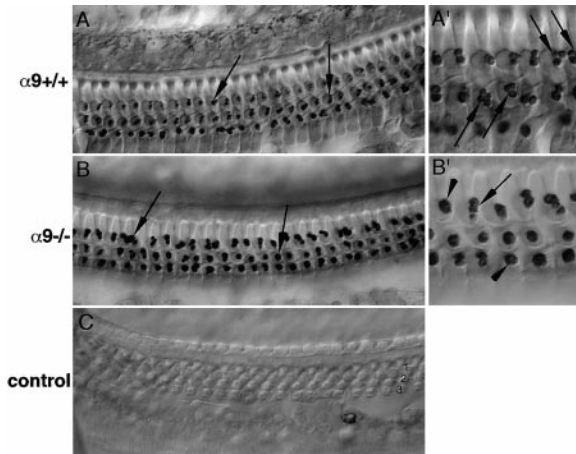


Figure 5. Vesicular Acetylcholine Transporter Immunostaining
Extensive cholinergic innervation to the organ of Corti persists in the $\alpha 9$ knockout mice.
(A) Immunohistochemistry using antibodies to vesicular acetylcholine transporter reveals cholinergic terminals within the organ of Corti of wild-type mice. Arrows point to small, efferent terminals under OHCs. Magnification, 630.
(A') High magnification reveals normal morphological features of efferent terminals under OHCs in wild-type mice. Arrows point to polyinnervated hair cells, one of which is contacted by four efferent terminals. The third row of hair cells is out of the plane of focus in this picture. Magnification, 1000.
(B) VAT immunostaining of cochleas from $\alpha 9$ knockout mice illustrate that cholinergic innervation persists in the knockout but that the efferent terminals under the OHCs are abnormal in their morphology. Three rows of large immunostained terminals can be seen under the three rows of OHCs. Magnification, 630.
(B') High magnification better reveals the abnormal VAT-positive efferent terminals found in the knockout mice as compared to those of the wild type. While some hair cells receive apparently normal complements of terminals (arrow), most were contacted by a single hypertrophied terminal (arrowheads). The hypertrophied terminals showed no bias as to their association with any specific row of hair cells.
(C) Section of the organ of Corti isolated from a wild-type mouse. No primary antibody was used in the immunostaining reaction. Numbers indicate rows of OHCs. Magnification, 630.

DPOAEs when presented with two simultaneous tones. One of the largest is at $2f_1-f_2$ (where f_1 and f_2 are the frequency values of the two primaries); this DPOAE is present in the vibrations of the basilar membrane (Ruggero et al., 1992) and requires normal OHCs to be produced. The emission is propagated from the inner ear (where it is produced), back through the ossicles to the ear canal, where it can be measured in the sound pressure waveform (Probst et al., 1991; Lonsbury-Martin et al., 1997). CAPs, on the other hand, represent the summed activity of cochlear afferent fibers discharging synchronously and thus assess the combined functional state of OHCs, IHCs, and their primary afferent innervation. Both DPOAEs and CAPs can be used to assess the functional state of different cochlear regions by varying the frequency of the acoustic stimulus.

Cochlear responses in the absence of crossing OC bundle stimulation were normal in homozygous and heterozygous knockouts, as compared with wild-type littermates. Assessments included measures of CAP threshold sensitivity across much of the normal hearing

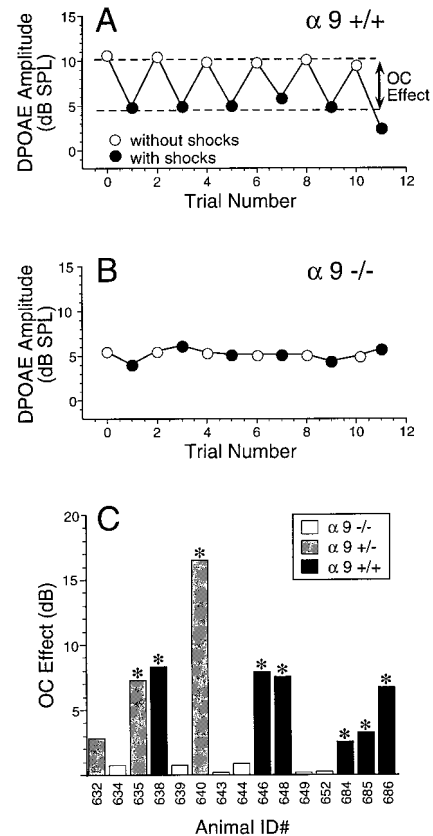


Figure 6. DPOAE-Based Assay of OC Effects

(A and B) DPOAE-based assay of classic OC effects on the cochlea in a typical wild type (A) and $\alpha 9$ knockout (B) mouse. Two tones (f_1 and f_2) were presented to the ear, and the resulting ear canal sound pressure was analyzed. The amplitude of the DPOAE at the frequency $2f_1-f_2$ was measured, first without (open circles) and then with (closed circles) simultaneous electric stimulation of OC fibers in the brainstem. This pair-wise comparison was then repeated five more times, for a total of 12 measurements. The absolute value of difference between the mean DPOAE amplitudes with versus without shocks is a measure of the magnitude of the OC effect on the cochlea. The 5 dB difference in the no-shocks DPOAE amplitude in the two examples represents normal interanimal variability. Noise floor was approximately -5 dB SPL.

(C) Results of a DPOAE-based assay of olivocochlear effects in each of the 15 animals tested in the present study. The OC effect is measured as described above. The f_2 frequency was either 18 or 20 kHz in all cases. In each animal, the assay was run multiple times, at a variety of f_2 SPLs between 35 and 65 dB. For each case, the level producing the maximal OC effect was chosen for display in this figure (SPLs used for the displayed set ranged from 45 to 60 dB, which produce a DPOAE 10–15 dB above the noise floor). Statistically significant OC effects ($p < 0.001$ in all cases) are indicated by asterisks above the bar. Animal ID number (x axis) also indicates the order in which the experiments were performed; thus, the only nonknockout in which a significant OC effect was not seen (animal 632) was the first experiment in the series. Animal genotype is indicated as described in the key.

range of the mouse (2–50 kHz), as well as measures of the growth of both CAPs and DPOAEs with increasing stimulus level at a number of stimulation frequencies. Cochlear responses in the knockouts are dealt with at greater length elsewhere (Liberman et al., 1999, Assoc. Res. Otolaryngol. Abs.).

We applied an assay for OC effects on the cochlear

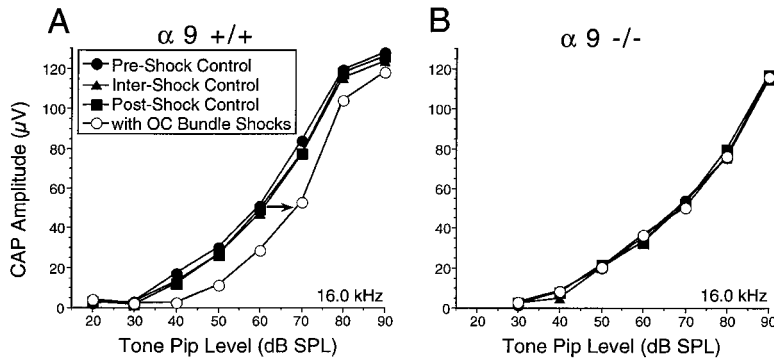


Figure 7. CAP-Based Assay of OC Effects
(A and B) Results of a compound-action potential-based assay of OC effects in a wild type (A) and a knockout (B). For this assay, the magnitude of the OC effect is estimated by comparing the CAP amplitude versus level function with and without OC shocks. For these cases, tone pip frequency was 16 kHz. Pips are presented at 4/s; 64 responses are averaged at each sound pressure level (SPL); and SPL is raised in 5 dB steps from sub-threshold levels to 90 dB SPL. At each SPL, measurements with and without MOC shocks are interleaved (to control for slow, or cumulative effects of OC stimulation) (Sridhar et al., 1995; Dallos et al., 1997). When present,

OC shocks consist of a train of 100 shocks (300/s) terminating 10 ms before each tone pip. The magnitude of the OC effects (arrow) is defined as an effective attenuation (Puria et al., 1996), i.e., the OC-induced shift (in dB) of the CAP amplitude versus level function along the level axis.

periphery by electrically stimulating the OC bundle at a midline point on the floor of the fourth ventricle, an area to which the OC fibers have ascended from their cell bodies of origin in the superior olivary complex and where some of the fibers cross the midline. Simultaneous with electrical stimulation, DPOAEs or CAPs were recorded. Most experiments used the DPOAE assay, since this measurement does not require the delicate surgery necessary to record the CAP. Our results demonstrate that classical OC function (as defined by results observed following midline activation of, presumably, mostly medial OC system fibers) in $\alpha 9$ knockout mice is severely compromised.

In wild-type controls, OC shock trains always caused clear and systematic alterations in DPOAE amplitude (Figure 6A). Primary tones were presented continuously ($f_2 = 18$ kHz) at a sound pressure level adequate to produce a DPOAE amplitude 10–20 dB above the measurement noise floor (in the absence of OC shocks). Six consecutive paired measurements were made in which the DPOAE was measured alternately without, and then with, simultaneous delivery of a continuous train of shocks. In the example shown in Figure 6A, the shock trains caused roughly a 5 dB decrease in DPOAE amplitude. In the knockout, by comparison, there was no apparent OC effect (Figure 6B). Given that the OC bundle remains intact in the knockout mice, failure to elicit a response cannot be due to the lack of (or misdirection of) the OC bundle that would lead to an unsuccessful stimulation of the fibers.

Data from all mice tested demonstrates that ablation of the $\alpha 9$ gene completely eliminates OC effects on the DPOAEs (Figure 6C). In each animal tested, a mean OC effect was computed from the six paired measurements, and the statistical significance of the difference was assessed (t test). All six wild-type control animals, and two out of three heterozygotes tested, showed a highly significant OC effect ($p < 0.001$). In contrast, none of the six knockouts tested showed an OC effect that was statistically significant (Figure 6C). Although only a few heterozygotes were tested, the data suggest no difference between wild types and heterozygotes with respect to the size of the OC effect. The average OC effect was compared between four wild-type and four knockout mice, all of which were closely matched for

frequencies and intensities used to elicit the DPOAE. The differences were statistically significant beyond the $p < 0.001$ level.

Knockout of the nAChR $\alpha 9$ subunit also eliminated OC effects on the CAP. In two knockouts, one wild type and one heterozygote, OC effects were assayed by comparing CAP amplitudes, as a function of stimulus level, with or without OC shocks. In the wild type and heterozygote, a classic OC effect was always observed (one example appears in Figure 7A). Thus, the CAP amplitude was always reduced by OC shocks, especially at low stimulus levels, resulting in a rightward shift of the level versus amplitude function, comparable to a 10 dB attenuation in sound level. In the knockouts, on the other hand, the shocks had no effect on CAP amplitudes. One example is shown in Figure 7B.

Discussion

The $\alpha 9$ Nicotinic Receptor Subunit and Development of Efferent Innervation

The abnormal efferent innervation in both OHC and IHC regions of the $\alpha 9$ nicotinic receptor knockout mouse suggests that the $\alpha 9$ subunit plays a role in the development of synaptic connections between efferent nerve fibers and hair cell somata. Abnormal target innervation resulting from loss of neurotransmitter receptors has also been reported in the NMDAR1 knockout mouse, where gene deletion caused malformations of barrelettes in the trigeminal nucleus (Li et al., 1994).

The elucidation of the exact mechanism(s) underlying the abnormal efferent terminal morphology is beyond the scope of this initial report characterizing the broad range of effects following ablation of the $\alpha 9$ gene. However, a few possible ways by which the abnormal morphology could come about can be envisioned. Mechanisms underlying the abnormalities in the $\alpha 9$ knockout may be analogous to those reported for the neuromuscular junction (Balice-Gordon and Lichtmann, 1994) where relative synaptic activity level has been shown to influence survival of different branches of a single motoneuron. This model would therefore predict that incoming fibers are capable of sampling target structures and assessing if the target is able to respond to a stimulus from the efferent fiber. In the absence of a

response, the fiber can sample other, nonconventional targets to find a responsive postsynaptic element, with the imbalance in activity leading to retraction of fibers from the silent target. In the IHC area, OC fibers normally target both IHC somata (although rarely) and the peripheral processes of type I spiral ganglion cells. Type I spiral ganglion neurons express nAChR subunits other than $\alpha 9$ (Morley et al., 1998) and thus presumably remain capable of responding to ACh and interacting with developing OC fibers in the knockout. Due to the lack of functional $\alpha 9$, the IHC presumably is not an ACh-responsive target. Following the logic of this model, this condition would then lead to the retraction of OC fibers from the silent IHCs, but the maintenance of the synaptic contacts with the ganglion cell processes. The OHCs, on the other hand, are innervated by afferent fibers from type II spiral ganglion neurons, which express only a low, possibly nonphysiological, level of the $\beta 2$ nAChR subunit (Morley et al., 1998). Except for a rare example (Xie et al., 1994), type II spiral ganglion cell processes do not express AChE, considered a marker for cholinergic targets. For these reasons, type II processes may not represent a viable alternative target capable of responding to ACh release from OC fibers. In the absence of mismatched postsynaptic target activity, due to the lack of an alternative ACh responsive target, there would be no retraction from the OHC somata, much as reported by Balice-Gordon and Lichtmann (1994) with a global neuromuscular junction block with α -bungarotoxin. However, it is clear that axo-dendritic synaptic contacts do exist between efferent and afferent fibers within the tunnel of Corti, at least in cats (Ginzberg and Morest, 1984). But the neurochemical phenotype of these efferent fibers remains unknown, and it is unclear whether a potential cholinergic region on these fibers far removed from the active zone of the hair cell and expressing nicotinic receptor subunits other than $\alpha 9$ would represent a viable alternate target for an efferent fiber growth cone normally contacting the hair cell somata. Clearly, more work must be done to establish whether this model is correct.

An alternate explanation may exist for the abnormal morphology of OC terminals in the OHC area. One may hypothesize that synaptic activity normally mediated by $\alpha 9$ regulates the expression of genes involved in cell adhesion. If, in the $\alpha 9$ knockout, the expression of these genes is not properly regulated, there might be abnormal adhesion between the incoming growth cone and the hair cell soma, along with a delay or absence of differentiation of the growth cone to a mature synaptic bouton. One candidate could be the expression of polysialic acid-decorated neural cell-adhesion molecule (PSA-NCAM). Indeed, blockage of nerve-induced activity has been shown to alter NCAM expression in developing chick myotubes (Fredette et al., 1993). Synaptic activity via AMPA-type glutamate receptors also regulates NCAM gene expression levels (Holst et al., 1998). It has been shown that PSA-NCAM expression decreases around the time when OC fibers are contacting their cochlear targets (Whitlon and Rutishauser, 1990; Whitlon and Zhang, 1997). The fact that singlet terminals on OHCs of wild-type and knockout mice were of equal size suggests that activity through the $\alpha 9$ channel is not capable of influencing final terminal size, or even target

recognition. Without $\alpha 9$ activity, the first terminal to contact an OHC enjoys an advantage in the competition for synaptic space on the soma it contacts, possibly because of a lack of adhesion between the growth cone and the hair cell, thereby allowing the efferent terminal to hypertrophy around the OHC soma.

Finally, in contrast to the possibility that activity via $\alpha 9$ exerts an influence on gene expression levels in the postsynaptic target (i.e., the hair cell), a lack of $\alpha 9$ activity may result in the loss of a more active interaction between the hair cell and maturing efferent terminal. Thus, one may postulate that with the lack of $\alpha 9$ activity, no diffusible retrograde message, as opposed to the cell adhesion "message," is sent back to the presynaptic terminal as a signal that an appropriate region on the target cell has been contacted. This hypothesis may predict that the synaptic contact between hair cell soma and efferent fiber remains in an immature, or undifferentiated, state longer than normal. This hypothesis can be tested by examining the expression of such molecular markers as GAP-43 to assess the length of time the efferent fibers spend in an undifferentiated state, followed by an examination of expression of known diffusible messengers such as NO.

The $\alpha 9$ Nicotinic Receptor Subunit and Olivocochlear Function

All hair cell systems, including auditory, vestibular, and lateral line organs, possess an efferent innervation of the receptor epithelium. The basic organization of a dual system differentially innervating the IHC and OHC regions applies to almost all mammalian species (White and Warr, 1983; Robertson, 1985; Thompson and Thompson, 1986; Aschoff et al., 1988; Aschoff and Ostwald, 1988; Campbell and Henson, 1988), the only known exception being one species of bat that appears to lack a medial OC innervation of OHCs. (Aschoff and Ostwald, 1987). The mammalian OC system contains both GABAergic and peptidergic components in addition to cholinergic components (for review, see Eybalin, 1993). Thus, mice with a targeted disruption of the $\alpha 9$ gene provide a molecular means of inactivating one neurochemically distinct OC subsystem among the multiple neurotransmitter components of this complex pathway.

In mammals, including humans, the medial OC subsystem innervating the OHCs constitutes a sound-evoked reflex pathway that is excited by sound in either ear (Folsom and Owsley, 1987; Liberman, 1989). In all species investigated, electric activation of the OC system decreases cochlear sensitivity, as measured either via afferent responses (Galambos, 1956; Desmedt, 1962), hair cell receptor potentials (Brown et al., 1983; Brown and Nuttall, 1984), DPOAEs (Mountain et al., 1980; Siegel and Kim, 1982), or basilar membrane motion (Murugasu and Russell, 1996). The functional utility of this reflex feedback pathway controlling cochlear thresholds, however, remains controversial. A number of different hypotheses have been suggested, including that it is: (1) a gain-control system to improve the detection of signals in noise (May and McQuone, 1995; Heinz et al., 1998; Winslow and Sachs, 1988); (2) a means of protecting the inner ear from acoustic overstimulation (Cody and Johnstone, 1982); and (3) a mechanism to mediate selective attention, for example, to visual over auditory stimuli, or to

high- versus low-frequency acoustic inputs (Oatman, 1971; Scharf et al., 1987, 1994).

There is evidence that classic OC suppression of cochlear thresholds is due exclusively to activation of medial OC fibers terminating on OHCs (Guinan et al., 1983). It has been further suggested that these OC effects are mediated by a receptor made up, at least in part, by $\alpha 9$ subunits (Elgoyhen et al., 1994), based on the similar pharmacological profiles seen in vivo (Desmedt and Monaco, 1961; Bobbin and Konishi, 1974; Fex and Adams, 1978; Kujawa et al., 1993, 1994) and in vitro (Housley and Ashmore, 1991; Fuchs and Murrow, 1992; Elgoyhen et al., 1994; Erostequi et al., 1994). The present results demonstrate that a loss of the $\alpha 9$ nAChR subunit leads to complete functional deafferentation, in the sense that classic effects of electrically shocking the OC bundle are completely absent in the knockout mouse (Figures 6 and 7). Furthermore, given that spiral ganglion neurons, the principal targets of the lateral OC subsystem, do not express $\alpha 9$ (Elgoyhen et al., 1994; Morley et al., 1998), the results support the notion that classic OC effects are mediated exclusively by the medial OC innervation of OHCs. Thus, the functional effects of activating the lateral OC system remain unknown.

In addition to influencing cochlear processing on a millisecond time scale, there is evidence that the OC system plays an important role in the development of OHCs. It has been shown that neonatal surgical deafferentation in cats causes permanent threshold elevations and other cochlear response abnormalities consistent with OHC dysfunction (Walsh et al., 1998). Such anomalies are not seen following surgical deafferentation in the adult (Warren and Liberman, 1989; Liberman, 1991), suggesting a critical period for OC involvement. The apparent normality of the cochlear responses in the $\alpha 9$ knockout mice (Liberman et al., 1999, Assoc. Res. Otolaryngol. Abs.) suggests that if the efferent system is involved in the functional development of OHCs, such an effect is mediated by a system that does not involve the $\alpha 9$ nicotinic receptor.

Conclusions

We have presented evidence that the $\alpha 9$ nACh receptor subunit plays a role in developing normal synaptic connections between efferent fibers and hair cells. Given that the normal relationship between the efferent fiber and the hair cell is stereotypic and common across many species, the efferent fiber-hair cell synapse may serve as a model for investigating synapse-target interactions and the mechanisms by which growth cones recognize targets and initiate conversion to a mature synaptic terminal. We have also shown that the $\alpha 9$ subunit is required for the classic suppressive effects of the olivocochlear efferent pathway on cochlear responses. Without $\alpha 9$, animals are functionally deafferented. Such a result is consistent with the normal expression of $\alpha 9$ by OHCs and the known role of OHCs in amplifying cochlear vibrations.

Experimental Procedures

Targeting Vector Construction and Generation of $\alpha 9$ -Deficient Mice

Two overlapping genomic clones spanning the entire coding sequence of the $\alpha 9$ subunit gene were isolated from a λ DASH II and

λ FIX II mouse genomic libraries prepared from 129/Sv mouse DNA (kindly provided by Dr. B. Bettler, Novartis, Basel). The intron-exon structure of the $\alpha 9$ gene was determined through genomic mapping, Southern blot analysis, and sequencing of the genomic clones. A 9.5 kb fragment of the λ FIX II genomic clone was subcloned into pBluescript SK⁺ and was used to generate the targeting construct (Figure 1A). The NcoI-EcoRV fragment coding for the entire exon 4 and flanking intronic sequences was replaced by a neomycin resistance gene (complete with its own stop codon) under the control of the pGK promoter. Additionally, the herpes simplex thymidine kinase gene, under the control of the MC1 promoter, was linked to the construct at the 5' HindIII site (Figure 1A). The resultant targeting vector was linearized at the 3' end prior to electroporation into the W9.5 embryonic stem (ES) cell line (Szabo and Mann, 1994). The methods for cell culture and transfection have been described previously (Köntgen and Stewart, 1993; Stewart, 1993; Vetter et al., 1996). Following electroporation and selection, embryonic stem cell clones were screened by Southern blot hybridization for proper recombination using a probe 3' annealing downstream to the site of recombination. Approximately 1 in 20 clones underwent correct homologous recombination. These clones were expanded without selection. Two of the clones were injected into blastocysts derived from the 129/SvEv mouse strain to produce chimeras, and these chimeras were then mated to CBA/CaJ or 129/SvEv mice in order to establish the $\alpha 9$ knockout genotype on several backgrounds. Germline transmission was confirmed by Southern blot analysis of DNA isolated from tail biopsies. The mutation has been maintained (via backcrossing to F6 generation at present) on either a CBA/CaJ, a crossed CBA/CaJ \times 129/SvEv, or a 129/SvEv background. No differences resulting from the various genetic backgrounds in any experiments reported in this manuscript have been observed.

Detection of $\alpha 9$ Transcripts by RT-PCR Analysis

Olfactory epithelia was isolated from either heterozygous or homozygous $\alpha 9$ knockout mice. Total RNA was isolated using guanidinium isothiocyanate as previously described (Chomczynski and Sacchi, 1987). First strand cDNA synthesis was accomplished using Superscript II reverse transcriptase (Life Technologies). An aliquot of 50 ng of cDNA was used as template for the PCR reactions. The following primers were used to amplify $\alpha 9$ transcripts: A903 (GenBank accession number U12336; nt 425–448, 5'-TGGAGGCCGACATTGTCC TATAC-3'), A904 (nt 995–1018, 5'-GATCAAGCCATGGTAGCTAT GTA-3'). Based on the rat $\alpha 9$ gene structure (Elgoyhen et al., 1994), a 594 bp PCR product is expected if exon 4-containing transcripts are expressed in the olfactory epithelium, and a fragment size of 61 base pair is predicted if exon 4 has been deleted (see Figure 1C). Amplification from genomic DNA would result in a fragment of approximately 7.5 kbp. Additionally, RT-PCR analysis for the presence of olfactory marker protein (OMP) transcripts was performed on the samples used for the analysis of $\alpha 9$ transcripts. The primers were as follows: OMP1 (GenBank accession number U01213; nt 879–897, 5'-AGCACTTGGCCATGGCAGAGGAT-3') and OMP2 (nt 1356–1379, 5'-GAGCTGGTTAAACACCACAGAGGC-3'). The predicted PCR fragment size is 501 bp (see Figure 1C). PCR reactions were performed as follows: 2.5 U HotStarTaq DNA polymerase (Qiagen), 0.5 μ M of each primer, 500 μ M each of dATP, dGTP, dCTP, and dTTP, and 2.5 mM MgCl. HotStarTaq PCR buffer and supplemental Q solution were added from stocks following supplier recommendations. Cycle parameters were: 15 min at 95°C followed by 34 cycles each of 1 min at 55°C, 1 min at 72°C, 30 s at 94°C, and a final cycle of 5 min at 55°C and 10 min at 72°C.

Morphological Assessments

For all histological procedures, mice were perfused transcardially with 4% paraformaldehyde, and the cochleas were removed and decalcified by overnight immersion in PBS-buffered 8% EDTA. For routine histological overview, cochleas were embedded in paraffin and sections were cut at 5–15 μ m and stained with hematoxylin and eosin. To evaluate innervation patterns in the cochlea, immunohistochemical methods were used. Decalcified cochleas were stripped of bone, and the organ of Corti was dissected into individual turns and then immunostained and viewed as surface preparation whole mounts. A polyclonal antibody against synaptophysin (gift

from Dr. R. Jahn; final dilution 1:1000) was used to visualize efferent innervation of hair cells, while a polyclonal antibody to vesicular acetylcholine transporter (Chemicon; final dilution 1:1000) was used to examine the cholinergic innervation. Antibody binding was revealed with either immunofluorescence or avidin-biotin DAB techniques. With immunofluorescence, tissue was examined with a Zeiss Axioplan 2 confocal microscope setup. All confocal illustrations are complete Z series stacks made through the subject being examined. A quantitative analysis of the efferent innervation to outer hair cells in wild-type and knockout mice was performed. Synaptophysin labeled efferent terminals in the middle turn of the cochlea were counted under 539 outer hair cells of wild-type mice and 859 outer hair cells of knockout mice. The multiplicity of efferent terminals was assessed by examining the terminal cluster under the outer hair cells through all focal planes. Most times, the number of terminals under the hair cells was easily assessed, but since this initial evaluation is done at the light microscopic level, there remains the chance that some single terminal profiles are actually multiple terminals, the individuality of which cannot be resolved by the light microscope. Electron microscopic analysis will better answer such concerns but is beyond the scope of this initial, broad-based investigation. Counts of terminals were tabulated as number of terminals per hair cell, and at least four mice of each genotype were used in this analysis. Data were binned as frequency of single, double, triple, etc., terminals observed under outer hair cells and used to create an observation frequency histogram. Additionally, total numbers of terminals were counted under OHCs from the middle turn, and a t test was performed to assess whether differences in the total number of efferent terminals was significantly different between genotypes. Statistical significance was assumed at $p < 0.05$. To assess the location of the OC bundle, several mice were perfused, and the auditory brainstem was isolated. Following standard procedures for cryosectioning, immunostaining was performed using antibodies to choline acetyltransferase (gift from Dr. C. Cozzari; final dilution 1:500) to localize cholinergic nerve fibers and cell bodies. All procedures were approved by the IACUC of the Salk Institute for Biological Studies.

Assessment of Cochlear Function

Nineteen mice, aged 6–24 weeks and of either sex, were tested, including knockouts as well as heterozygous and wild-type littermates. All procedures were approved by the IACUC of both the Massachusetts Eye and Ear Infirmary and the Salk Institute for Biological Studies.

Anesthesia and Surgery

Mice were anesthetized with xylazine (5 mg/kg intraperitoneally) and urethane (1.2 mg/g intraperitoneally). A tracheostomy was performed, and the pinna was removed. The OC bundle was exposed at the floor of the fourth ventricle by removing occipital bone and dura followed by cerebellar aspiration. When compound action potentials (CAPs) were to be recorded, the bulla was exposed and opened with a scalpel, revealing the round window of the cochlea. Body temperature was maintained near 37°C by varying ambient air temperature.

Stimulation of the OC Bundle

Following aspiration of a portion of the cerebellum, a three-tined rake of silver wires (0.5 mm spacing) was inserted into the dorsal surface of the brainstem, along the midline, at an anterior-posterior location spanning the decussation of the OC bundle (judged via surface landmarks such as the facial genua). Trains of monophasic 150 μ s pulses (150–300/s) were delivered to different wire pairs, while varying shock-train amplitude and observing facial twitches. The electrode pair eliciting twitches at the lowest shock level was selected (the OCB runs close to the facial nerve); the animal was then paralyzed (tubocurarine, 4 mg/kg) and connected to a ventilator through the tracheostomy tube. After paralysis was complete, the shock amplitude was raised by 12 dB and lack of facial twitching was verified (testing was usually carried out at 6 dB above twitch threshold).

Distortion Product Otoacoustic Emissions (DPOAEs)

DPOAEs were measured from the ear canal with an ER-10c probe system (Etymotics Research) and linked D-A and A-D boards in a Macintosh running custom LabVIEW software (National Instruments,

Texas). Two pure tones (f_1 and f_2 ; $f_2/f_1 = 1.2$) were synthesized (National Instruments AO6 D-A board) and presented to the ear canal (with f_2 level always 10 dB $>$ f_1) via the two transducers in the ER-10C. Resultant ear canal sound pressure was transduced by the calibrated microphone in the ER-10C system, then amplified, filtered (1000 Hz high-pass), and digitized (National Instruments A2000 A-D board). A fast Fourier transform (FFT) was performed, and the amplitude of the distortion component at $2f_1 - f_2$ was computed, as was the noise floor (average of six frequency bins on either side of $2f_1 - f_2$). Noise floor was not statistically different between mice genotypes and, therefore, has not been included in the graphs of DPOAE amplitudes. System distortion was monitored by measuring $2f_1 - f_2$ in a passive coupler. To assess OC function, DPOAE amplitudes were compared with and without simultaneous (and continuous) electric stimulation of the OC bundle.

Compound Action Potentials (CAPs)

CAP was recorded via a silver wire on the round window membrane, referred to the mouthbar, amplified (10,000 \times), filtered (0.3 to 3 kHz passband), digitized, and averaged. Acoustic stimuli were 5 ms tone pips (0.5 ms rise-fall) presented at 4/s through one of the ER-10C transducers. Responses to 64 stimuli were averaged, with stimulus polarity reversed on half of the presentations to remove cochlear microphonic potentials. To assess OC function, CAP amplitudes were compared with and without electric stimulation of the OC bundle, delivered in a 100 ms bursts, each burst ending 10 ms before each tone pip.

Acknowledgments

This work was supported by grants from NIDCD, DC02871 (S. F. H.), and DC00188 (M. C. L.). Additional funding was provided by the Adler Foundation (S. F. H.). Funding to A. B. E. is through an International Research Scholar grant (Howard Hughes Medical Institute), Strauss Foundation Award in Auditory Science, and a Fogarty International Research Collaboration.

Received March 16, 1999; revised April 5, 1999.

References

- Aschoff, A., and Ostwald, J. (1987). Different origins of cochlear efferents in some bat species, rats, and guinea pigs. *J. Comp. Neurol.* 264, 56–72.
- Aschoff, A., and Ostwald, J. (1988). Distribution of cochlear efferents and olivo-collicular neurons in the brainstem of rat and guinea pig. A double labeling study with fluorescent tracers. *Exp. Brain Res.* 71, 241–251.
- Aschoff, A., Muller, M., and Ott, H. (1988). Origin of cochlea efferents in some gerbil species. A comparative anatomical study with fluorescent tracers. *Exp. Brain Res.* 71, 252–261.
- Balice-Gordon, R.J., and Lichtmann, J.W. (1994). Long-term synapse loss induced by focal blockade of postsynaptic receptors. *Nature* 372, 519–524.
- Bobbin, R.P., and Konishi, T. (1974). Action of cholinergic and anticholinergic drugs at the crossed olivocochlear bundle-hair cell junction. *Acta Otolaryngol. (Stockh.)* 77, 56–65.
- Brown, M.C., and Nuttall, A.L. (1984). Efferent control of cochlear inner hair cell responses in the guinea-pig. *J. Physiol. (Lond.)* 354, 625–646.
- Brown, M.C., Nuttall, A.L., and Masta, R.I. (1983). Intracellular recordings from cochlear inner hair cells: effects of stimulation of the crossed olivocochlear efferents. *Science* 222, 69–72.
- Campbell, J.P., and Henson, M.M. (1988). Olivocochlear neurons in the brainstem of the mouse. *Hear. Res.* 35, 271–274.
- Chomczynski, P., and Sacchi, N. (1987). Single-step method of RNA isolation by acid guanidinium thiocyanate-phenol-chloroform extraction. *Anal. Biochem.* 162, 156–159.
- Cody, A.R., and Johnstone, B.M. (1982). Acoustically evoked activity of single efferent neurons in the guinea pig cochlea. *J. Acoust. Soc. Am.* 72, 280–282.
- Dallos, P., He, D., Lin, X., Sziklai, I., Mehta, S., and Evans, B. (1997).

- Acetylcholine, outer hair cell electromotility, and the cochlear amplifier. *J. Neurosci.* *17*, 2212–2226.
- Desmedt, J. (1962). Auditory-evoked potentials from cochlea to cortex as influenced by activation of the efferent olivocochlear bundle. *J. Acoust. Soc. Am.* *34*, 1478–1496.
- Desmedt, J., and Monaco, P. (1961). Mode of action of the efferent olivo-cochlear bundle on the inner ear. *Nature* *192*, 1263–1265.
- Elgoyhen, A.B., Johnson, D.S., Boulter, J., Vetter, D.E., and Heinemann, S. (1994). Alpha 9: an acetylcholine receptor with novel pharmacological properties expressed in rat cochlear hair cells. *Cell* *79*, 705–715.
- Emmerling, M.R., Sobkowicz, H.M., Levenick, C.V., Scott, G.L., Slapnick, S.M., and Rose, J.E. (1990). Biochemical and morphological differentiation of acetylcholinesterase-positive efferent fibers in the mouse cochlea. *J. Electron Microsc. Tech.* *15*, 123–143.
- Erostegui, C., Norris, C.H., and Bobbin, R.P. (1994). In vitro pharmacologic characterization of a cholinergic receptor on outer hair cells. *Hear. Res.* *74*, 135–147.
- Eybalin, M. (1993). Neurotransmitters and neuromodulators of the mammalian cochlea. *Physiol. Rev.* *73*, 309–373.
- Fex, J., and Adams, J.C. (1978). Alpha-Bungarotoxin blocks reversibly cholinergic inhibition in the cochlea. *Brain Res.* *159*, 440–444.
- Folsom, R., and Owsley, R. (1987). N1 action potentials in humans. Influence of simultaneous contralateral stimulation. *Acta Otolaryngol. (Stockh.)* *103*, 262–265.
- Fredette, B., Rutishauser, U., and Landmesser, L. (1993). Regulation and activity-dependence of N-cadherin, NCAM isoforms, and polysialic acid on chick myotubes during development. *J. Cell Biol.* *123*, 1867–1888.
- Fritzsch, B., and Nichols, D.H. (1993). Dil reveals a prenatal arrival of efferents at the differentiating otocyst of mice. *Hear. Res.* *65*, 51–60.
- Fuchs, P.A., and Murrow, B.W. (1992). A novel cholinergic receptor mediates inhibition of chick cochlear hair cells. *Proc. R. Soc. Lond. B Biol. Sci.* *248*, 35–40.
- Galambos, R. (1956). Suppression of auditory nerve activity by stimulation of efferent fibers to the cochlea. *J. Neurophysiol.* *19*, 424–437.
- Ginzberg, R.D., and Morest, D.K. (1984). Fine structure of cochlear innervation in the cat. *Hear. Res.* *14*, 109–127.
- Glowatzki, E., Wild, K., Brändle, U., Fakler, G., Fakler, B., Zenner, H.-P., and Ruppersberg, J.P. (1995). Cell-specific expression of the $\alpha 9$ n-ACh receptor subunit in auditory hair cells revealed by single cell RT-PCR. *Proc. R. Soc. Lond. B* *262*, 141–147.
- Guinan, J.J., Jr., Warr, W.B., and Norris, B.E. (1983). Differential olivocochlear projections from lateral versus medial zones of the superior olivary complex. *J. Comp. Neurol.* *221*, 358–370.
- Hashimoto, S., Kimura, R.S., and Takasaka, T. (1990). Computer-aided three-dimensional reconstruction of the inner hair cells and their nerve endings in the guinea pig cochlea. *Acta Otolaryngol. (Stockh.)* *109*, 228–234.
- Heinz, R., Stiles, P., and May, B. (1998). Effects of bilateral olivocochlear lesions on vowel formant discrimination in cats. *Hear. Res.* *116*, 10–20.
- Hiel, H., Elgoyhen, A., Drescher, D., and Morley, B. (1996). Expression of nicotinic acetylcholine receptor mRNA in the adult rat peripheral vestibular system. *Brain Res.* *738*, 347–352.
- Holst, B., Vanderklish, P., Krushel, L., Zhou, W., Langdon, R., McWhirter, J., Edelman, G., and Crossin, K. (1998). Allosteric modulation of AMPA-type glutamate receptors increases activity of the promoter for the neural cell adhesion molecule, NCAM. *Proc. Natl. Acad. Sci. USA* *95*, 2597–2602.
- Housley, G.D., and Ashmore, J.F. (1991). Direct measurement of the action of acetylcholine on isolated outer hair cells of the guinea pig cochlea. *Proc. R. Soc. Lond. B Biol. Sci.* *244*, 161–167.
- Klinke, R., and Galley, N. (1974). Efferent innervation of vestibular and auditory receptors. *Physiol. Rev.* *54*, 316–357.
- Kontgen, F., and Stewart, C.L. (1993). Simple screening procedure to detect gene targeting events in embryonic stem cells. *Methods Enzymol.* *225*, 878–890.
- Kujawa, S.G., Glatcke, T.J., Fallon, M., and Bobbin, R.P. (1992). Intracochlear application of acetylcholine alters sound-induced mechanical events within the cochlear partition. *Hear. Res.* *61*, 106–116.
- Kujawa, S.G., Glatcke, T.J., Fallon, M., and Bobbin, R.P. (1993). Contralateral sound suppresses distortion product otoacoustic emissions through cholinergic mechanisms. *Hear. Res.* *68*, 97–106.
- Kujawa, S.G., Glatcke, T.J., Fallon, M., and Bobbin, R.P. (1994). A nicotinic-like receptor mediates suppression of distortion product otoacoustic emissions by contralateral sound. *Hear. Res.* *74*, 122–134.
- Lauder, J.M. (1993). Neurotransmitters as growth regulatory signals: role of receptors and second messengers. *Trends Neurosci.* *16*, 233–240.
- Li, Y., Erzurumlu, R.S., Chen, C., Jhaveri, S., and Tonegawa, S. (1994). Whisker-related neuronal patterns fail to develop in the trigeminal brainstem nuclei of NMDAR1 knockout mice. *Cell* *76*, 427–437.
- Lieberman, M.C. (1989). Rapid assessment of sound-evoked olivocochlear feedback: suppression of compound action potentials by contralateral sound. *Hear. Res.* *38*, 47–56.
- Lieberman, M.C. (1991). The olivocochlear efferent bundle and susceptibility of the inner ear to acoustic injury. *J. Neurophysiol.* *65*, 123–132.
- Lipton, S.A., Frosch, M.P., Phillips, M.D., Tauck, D.L., and Aizenman, D.L. (1988). Nicotinic antagonists enhance process outgrowth by rat retinal ganglion cells in culture. *Science* *239*, 1293–1296.
- Lonsbury-Martin, B.L., Martin, G.K., and Whitehead, M.L. (1997). Distortion product otoacoustic emissions. In *Otoacoustic Emissions: Clinical Applications*, M.S. Robinette and T.J. Glatcke, eds. (New York: Thieme), pp. 83–109.
- Luo, L., Bennett, T., Jung, H.H., and Ryan, A.F. (1998). Developmental expression of $\alpha 9$ acetylcholine receptor mRNA in the rat cochlea and vestibular inner ear. *J. Comp. Neurol.* *393*, 320–331.
- Mattson, M.P. (1988). Neurotransmitters in the regulation of neuronal cytoarchitecture. *Brain Res. Brain Res. Rev.* *13*, 179–212.
- May, B., and McQuone, S. (1995). Effects of bilateral olivocochlear efferent lesions on pure-tone intensity discrimination in cats. *Aud. Neurosci.* *1*, 385–400.
- Morley, B., Li, H., Hiel, H., Drescher, D., and Elgoyhen, A. (1998). Identification of the subunits of the nicotinic cholinergic receptors in the rat cochlea using RT-PCR and in situ hybridization. *Brain Res. Mol. Brain Res.* *53*, 78–87.
- Mountain, D.C. (1980). Changes in endolymphatic potential and crossed olivocochlear bundle stimulation alter cochlear mechanics. *Science* *210*, 71–72.
- Mountain, D.C., Geisler, C.D., and Hubbard, A.E. (1980). Stimulation of efferents alters the cochlear microphonic and the sound-induced resistance changes measured in scale media of the guinea pig. *Hear. Res.* *3*, 231–240.
- Murugasu, E., and Russell, I. (1996). The effect of efferent stimulation on basilar membrane displacement in the basal turn of the guinea pig cochlea. *J. Neurosci.* *16*, 325–332.
- Oatman, L. (1971). Role of visual attention on auditory evoked potentials in unanesthetized cats. *Exp. Neurol.* *32*, 341–356.
- Probst, R., Lonsbury-Martin, B.L., and Martin, G.K. (1991). A review of otoacoustic emissions. *J. Acoust. Soc. Am.* *89*, 2027–2067.
- Puria, S., Guinan, J.J., Jr., and Liberman, M. (1996). Olivocochlear reflex assays: effects of contralateral sound on compound action potentials versus ear-canal distortion products. *J. Acoust. Soc. Am.* *99*, 500–507.
- Rasmussen, G.L. (1942). An efferent cochlear bundle. *Anat. Rec.* *82*, 441.
- Rasmussen, G.L. (1946). The olivary peduncle and other fiber projections of the superior olivary complex. *J. Comp. Neurol.* *84*, 141–219.
- Rasmussen, G.L. (1955). Descending, or “feed-back” connections of the auditory system of the cat. *Am. J. Physiol.* *183*, 653.
- Robertson, D. (1985). Brainstem location of efferent neurones projecting to the guinea pig cochlea. *Hear. Res.* *20*, 79–84.
- Ruggero, M.A., Robles, L., Rich, N.C., and Recio, A. (1992). Basilar

- membrane responses to two-tone and broadband stimuli. *Philos. Trans. R. Soc. Lond. B Biol. Sci.* *336*, 307–314; discussion 314–135.
- Scharf, B., Quigley, S., Aoki, C., Peachey, N., and Reeves, A. (1987). Focused auditory attention and frequency selectivity. *Percept. Psychophys.* *42*, 215–223.
- Scharf, B., Magnan, J., Collet, L., Ulmer, E., and Chays, A. (1994). On the role of the olivocochlear bundle in hearing: a case study. *Hear. Res.* *75*, 11–26.
- Siegel, J.H., and Kim, D.O. (1982). Efferent neural control of cochlear mechanics? Olivocochlear bundle stimulation affects cochlear biomechanical nonlinearity. *Hear. Res.* *6*, 171–182.
- Slepecky, N. (1996). Structure of the mammalian cochlea. In *The Cochlea*, P. Dallos, A.N. Popper, and R.R. Fay, eds. (New York: Springer), pp. 44–129.
- Sobkowicz, H. (1992). The development of innervation in the organ of Corti. In *Development of the Auditory and Vestibular Systems 2*, R. Romand, ed. (New York: Elsevier Science Publishers), pp. 59–100.
- Sridhar, T., Liberman, M., Brown, M., and Sewell, W. (1995). A novel cholinergic “slow effect” of efferent stimulation on cochlear potentials in the guinea pig. *J. Neurosci.* *15*, 3667–3678.
- Stewart, C.L. (1993). Production of chimeras between embryonic stem cells and embryos. *Methods Enzymol.* *225*, 823–855.
- Szabo, P., and Mann, J.R. (1994). Expression and methylation of imprinted genes during in vitro differentiation of mouse parthenogenetic and androgenetic stem cell lines. *Development* *120*, 1651–1660.
- Thompson, G.C., and Thompson, A.M. (1986). Olivocochlear neurons in the squirrel monkey brainstem. *J. Comp. Neurol.* *254*, 246–258.
- Ulfendahl, M. (1997). Mechanical responses of the mammalian cochlea. *Prog. Neurobiol.* *53*, 331–380.
- Vetter, D.E., Mann, J.R., Wangemann, P., Liu, J., McLaughlin, K.J., Lesage, F., Marcus, D.C., Lazdunski, M., Heinemann, S.F., and Barhanin, J. (1996). Inner ear defects induced by null mutation of the *isk* gene. *Neuron* *17*, 1251–1264.
- Walsh, E., McGee, J., McFadden, S., and Liberman, M. (1998). Long-term effects of sectioning the olivocochlear bundle in neonatal cats. *J. Neurosci.* *18*, 3859–3869.
- Warren, E.H.D., and Liberman, M.C. (1989). Effects of contralateral sound on auditory-nerve responses. II. Dependence on stimulus variables. *Hear. Res.* *37*, 105–121.
- White, J.S., and Warr, W.B. (1983). The dual origins of the olivocochlear bundle in the albino rat. *J. Comp. Neurol.* *219*, 203–214.
- Whitlon, D.S., and Rutishauser, U.S. (1990). NCAM in the organ of Corti of the developing mouse. *J. Neurocytol.* *19*, 970–977.
- Whitlon, D.S., and Zhang, X. (1997). Polysialic acid in the cochlea of the developing mouse. *Int. J. Dev. Neurosci.* *15*, 657–669.
- Wiederhold, M.L., and Kiang, N.Y. (1970). Effects of electric stimulation of the crossed olivocochlear bundle on single auditory-nerve fibers in the cat. *J. Acoust. Soc. Am.* *48*, 950–965.
- Winslow, R.L., and Sachs, M.B. (1988). Single-tone intensity discrimination based on auditory-nerve rate responses in backgrounds of quiet, noise, and with stimulation of the crossed olivocochlear bundle. *Hear. Res.* *35*, 165–189.
- Xie, D.H., Henson, M.M., and Henson, O.W., Jr. (1994). AChE-staining of type II ganglion cells, processes and terminals in the cochlea of the mustached bat. *Hear. Res.* *75*, 61–66.